Generation of an optical vortex with a segmented deformable mirror

Robert K. Tyson, Marco Scipioni,* and Jaime Viegas

Department of Physics and Optical Science, University of North Carolina at Charlotte, 9201 University City Boulevard, Charlotte, North Carolina 28223, USA

*Corresponding author: mscipion@uncc.edu

Received 3 March 2008; revised 5 May 2008; accepted 28 October 2008; posted 29 October 2008 (Doc. ID 93346); published 20 November 2008

We present a method for the creation of optical vortices by using a deformable mirror. Optical vortices of integer and fractional charge were successfully generated at a wavelength of 633 nm and observed in the far field (2000 mm). The obtained intensity patterns proved to be in agreement with the theoretical predictions on integer and fractional charge optical vortices. Interference patterns between the created optical vortex carrying beams and a reference plane wave were also produced to verify and confirm the existence of the phase singularities. © 2008 Optical Society of America

OCIS codes: 050.4865, 260.0260, 030.7060, 070.7345, 350.4600.

1. Optical vortices

An optical vortex (also known as a screw dislocation or phase singularity) is a zero of an optical field, a point of zero intensity [1]. Light is twisted like a corkscrew around its axis of propagation [2,3]. Because of the twisting, the light waves at the axis itself cancel each other out. An optical vortex looks like a ring of light with a dark hole in the center. The vortex is given a number, called the topological charge ℓ, related to the orbital angular momentum of the field. The wavefront of an optical vortex is a continuous surface consisting of ℓ embedded helicoids, each with $\ell\lambda$ pitch, spaced from each other at one wavelength λ. As an example, Fig. 1 represents the wavefront of a charge $\ell = 3$ vortex propagating along the z axis, illustrating the three intertwined helicoids.

The generalized functional form for a field hosting an optical vortex is, in a plane transverse to propagation direction, locally given by

$$f(r,\theta) = A(r,\theta)e^{i\ell\theta}, \tag{1}$$

where $A(r,\theta)$ can be any square integrable, continuous, and smooth complex amplitude wave function in cylindrical polar coordinates. The phase argument θ represents the distinctive, transverse vortex phase profile, impressing a linear phase increase in the azimuthal direction to the field. The charge of a vortex can be an integer or fraction, and also be positive or negative, depending on the handedness of the twist. Figure 2 shows a map of the phase profile of a vortex beam. The phase jumps by a value $\ell 2\pi$ at the discontinuity.

Vortex beams have been successfully employed in optical tweezers applications [4–7] because they offer the advantage of trapping and spinning low index (with respect to the hosting medium) dielectric particles in their zero-intensity region.

Vortex carrying beams also have interesting potential for use in free-space optical communications [8–11]. Of particular interest is the ability of vortex beams to conserve their charge through atmospheric turbulence [12]. Also, vortex beams "self-heal" around obstacles [13] and experiments have shown that vortices are conserved through fog [14]. These properties make it an ideal extension to conventional coding schemes, such as on–off keying or coherent modulation techniques.

0003-6935/08/336300-07$15.00/0
© 2008 Optical Society of America

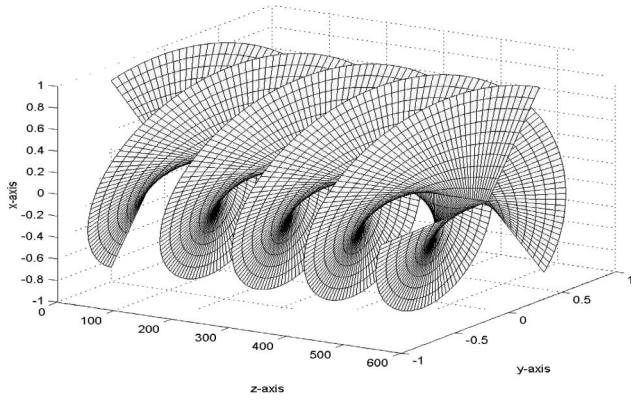

Fig. 1. Wavefront of an optical vortex with charge $\ell = 3$ (arbitrary spatial units).

2. Generation of an Optical Vortex

Optical vortices can be generated in a number of ways. We briefly review the methods here. Details of the methods and operation are found in the citations.

A. Spatial Light Modulator

One commonly used device for the generation of an optical vortex is the liquid-crystal spatial light modulator (LC SLM) [15]. Commercial LC SLMs are either optically or electrically addressed and can modulate the amplitude, the phase, or both, for an incident input field. Their main strength point is that they are dynamically reprogrammable. Nematic SLM, the most common, has a time response of roughly 60 Hz. When an SLM is used, any significant incident beam power must be distributed in order to avoid boiling the liquid-crystal element, so the amount of incident power can be a limitation.

In the case of amplitude-only spatial light modulators, an optical vortex of a given charge and wavelength can be made from a computer-generated hologram (CGH) [16]. CGHs are the digitally calculated interferograms between a plane wave beam and a beam carrying an optical vortex. The resulting CGH resembles a diffraction grating with a characteristic "fork" dislocation, with the number of prongs in the fork directly related to the topological charge of the design vortex (number of prongs = desired topological charge + 1). The CGH is then applied to the SLM.

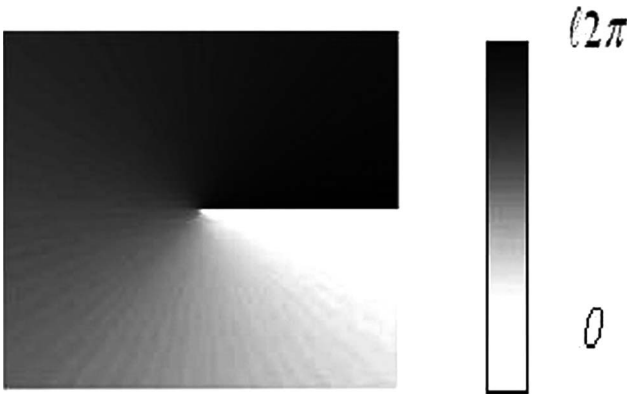

Fig. 2. Vortex phase in plane transverse to propagation.

In the case of phase-only SLMs, the phase profile is the sum of the desired optical vortex phase and a phase tilt needed to steer the reflected incident beam away from the direction of incidence. The result is a blazed phase grating that still has a fork feature in its center. Because the blazed phase grating is not perfect, multiple diffraction orders appear after the beam is reflected off the SLM. The first diffraction order contains the optical vortex with the desired topological charge and is the most intense diffraction order. The zero diffraction order is the specular reflection off the SLM. The other diffraction orders are vortex beams with topological charge equal to the diffraction order number multiplied by the topological charge of the desired vortex beam.

B. Mode Converters

Hermite–Gaussian laser modes form an orthogonal family of laser beams. An appropriately weighted superposition of two Hermite–Gaussian beams, with the right mode order, can result in a Laguerre–Gaussian beam carrying an optical vortex of the desired topological charge at its center. The superposition is achieved through a system of cylindrical lenses by making use of the Gouy effect [17]. This setup presents alignment challenges and requires high-order Hermite–Gaussian beams to obtain high-order vortex beams, thus limiting the flexibility of the configuration.

C. Helical Mirror

A helical mirror was recently proposed [18] to create optical phase singularities of various topological charges. The mirror shape, controlled by a piezoelectric actuator, provides a continuous phase variation along the azimuthal direction, but also introduces radial phase variations because of unavoidable material stresses, thus lowering the quality of the generated vortex beams.

D. Dielectric Wedges

By stacking dielectric wedges [19,20], it was shown to be possible to create a system capable of producing optical vortices of topological charge higher than one. The charge of the vortex beams corresponds to the number of wedges used in the system.

E. Spiral Phase Plates

A simple, adjustable spiral phase plate has also been used to create vortex beams [21]. The plate is constructed from a parallel-sided transparent plate with polished surfaces in which a crack is induced starting at one edge and terminating close to its center.

Static spiral phase plates (SPPs) are very common. They are spiral-shaped pieces of crystal or plastic that approximate the ideal spiral with a discrete number of phase steps. SPPs are engineered specifically to the desired topological charge and incident

wavelength [22–25]. They are efficient, yet expensive, and show high topological charge purity only for low topological charge ℓ [26].

F. Deformable Mirrors

A deformable mirror (DM) can be used to generate a vortex. A conventional continuous faceplate DM is not well suited for this action because the surface must have a discontinuous line (not necessarily straight) between the singularity and the edge. On the other hand, a segmented DM, with discontinuities already in place between the segments, can be formed into a vortex shape, which is transferred to the phase of a beam reflecting from the surface.

If, at the discontinuity, the surface jumps one-half of the wavelength of the light, the reflected beam will have a phase jump of one full wave and the beam will have a vortex charge $\ell = 1$. By simply multiplying the amplitudes of the segment pistons and tilts, we can apply any charge to the beam, up to the mechanical limits of the DM. This allows us a great variability of charge and even fractional charges. Because the mirror is simply a reflecting surface, it can be used at multiple wavelengths.

3. Results with a Segmented Deformable Mirror

We have performed a number of experiments with our 37-segment deformable mirror and have shown that we can generate a vortex. We can vary the charge and have verified the charge in the pupil plane and in the far field after propagation. The device used to demonstrate vortex generation is the Iris AO S37-X segmented deformable mirror [27]; see Fig. 3. The S37-X deformable mirror is fabricated with micromachining technology, making it a compact, low mass modulator. The 3.5 mm aperture DM consists of 37 hexagonal segments tiled into an array.

The DM segment consists of an actuator platform elevated above the substrate as a result of engineered residual stresses in the bimorph flexures. The actuator platform and underlying electrodes form parallel plate capacitors. Placing a voltage

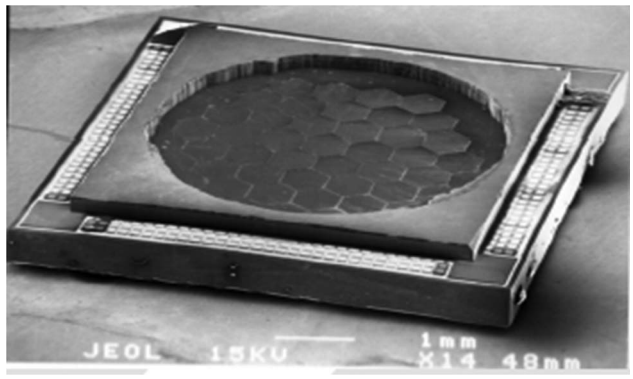

Fig. 3. Iris AO S37-X segmented deformable mirror.

across the capacitors generates Coulombic forces that pull the segment toward the substrate. By varying the voltages on the lower electrodes, the actuator can move in piston (pure vertical), tip, and tilt directions. The forces are solely attractive, so bidirectional actuation is achieved by biasing the segment at the halfway point.

Electrostatic actuation has a nonlinear response between position and voltage. Furthermore, the segment piston/tip/tilt positions are coupled, making the position versus voltage response more complicated. Iris AO has developed a controller that linearizes this response. The user simply enters desired piston/tip/tilt positions and the controller, using a calibrated model, determines the required voltages and sets them on the drive electronics. The controller has demonstrated open-loop positioning of 30 nm rms residual surface figure errors. Thus, a vortex can be created with the DM in open-loop operation.

Figure 4 shows the spiral ramp generated by the DM compared to the ideal, infinitely smooth spiral vortex ramp.

Beams carrying topological charge $|\ell| > 1$ are highly unstable to small symmetry-breaking azimuthal perturbations and decompose, upon propagation, into elementary charge $\ell = 1$ vortices of the same sign, symmetrically distributed around the

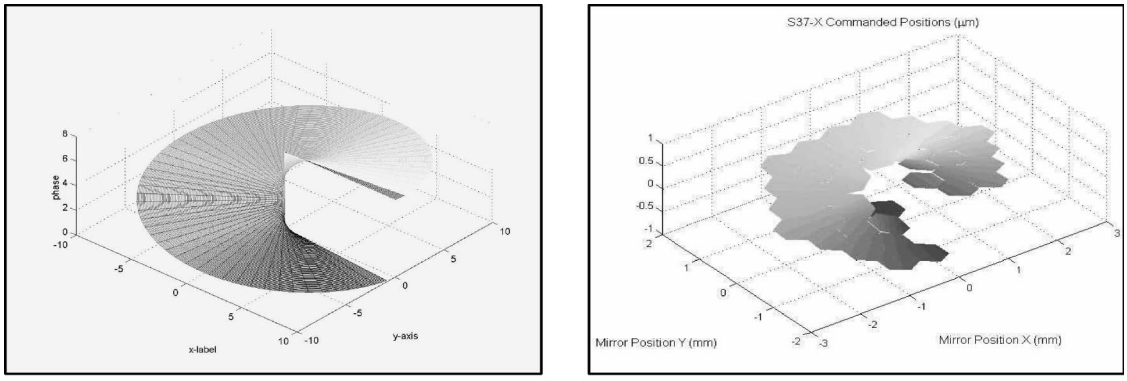

(a) (b)

Fig. 4. (a) Ideal linear spiral ramp and (b) ramp approximated by Iris AO deformable mirror.

center of the beam, thus conserving the initial net topological charge [28]. Astigmatism in the beam or small defects in the diffracting/reflecting optical device are the probable causes of this fragmentation.

Figure 5 illustrates the unfolding. A dipole in Fig. 5 (b), a tripole in Fig. 5(c), and a quadrupole in Fig. 5(d) are shown from the decay of charge two, three, and four optical vortex beams created with the Iris AO deformable mirror.

We also verified the optical charge from interference patterns in the pupil plane. The interference patterns between a reference plane wave and a beam carrying an optical vortex were generated by using a Michelson interferometer.

The resulting interference patterns shown in Fig. 6 reveal the typical fork pattern, which is an indicator of the presence of the phase singularities in the beam reflecting off the deformable mirror. In Fig. 6(b) the interference fringes represent the deformable mirror commanded to a flat profile. In Fig. 6(d) the two-pronged fork pattern for a charge 1 vortex is shown and in agreement with the simulation. For Fig. 6(f), we placed amplitudes on the deformable mirror that would generate a charge 5 optical vortex. The simulated and experimental patterns are different because, upon the short propagation length within the interferometer (a few centimeters), the charge 5 vortex apparently unfolded into five elementary charge 1 vortices, as expected. We interpret the interference pattern to be the presence of five two-pronged forks within the pattern, indicating the presence of a charge 5 vortex.

Optical vortices with half-integer topological charge exhibit, in the near field, a radial line of low intensity attributed to the presence of a chain of charge 1 vortices of alternating sign along the radial phase discontinuity [28,29].

In the far field, however, only a finite number of same-sign vortices appear near the beam axis [30,31]. The number results from rounding the fractional charge ℓ of the vortex to the nearest higher integer. For example, if $\ell = 0.5$, the far field will show one charge 1 vortex, and, similarly, three charge 1 vortices, if $2.5 \leq \ell < 3.5$.

In Fig. 7, each dark region indicates the presence of an optical vortex in the field. By increasing the height of the phase discontinuity in discrete increments, it is interesting to follow the evolution of the intensity of the beam as the discontinuity changes from one integer value of the wavelength to the next higher one. It is apparent from Fig. 7, as predicted from theory [31,32], that as the discontinuity passes a half-integer value of the wavelength λ, a new vortex fully appears in the beam, migrating

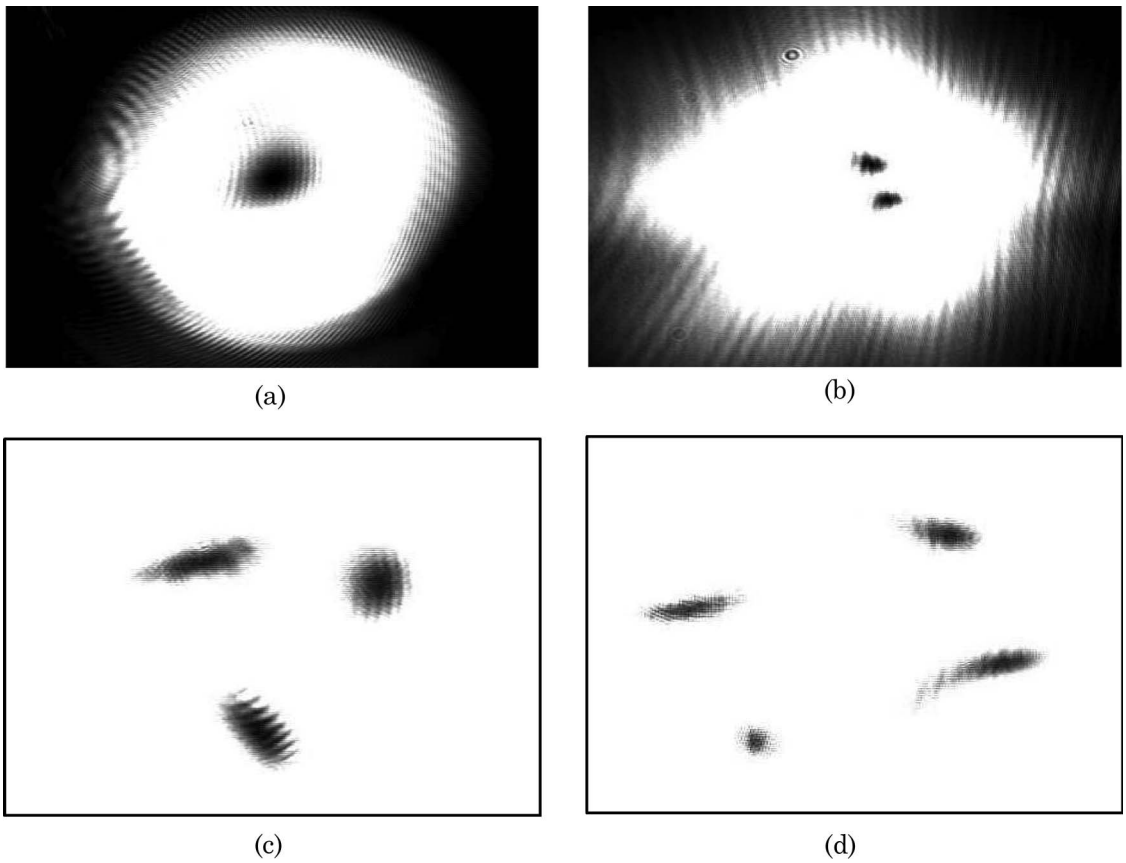

Fig. 5. Decay of multiple-charge optical vortices into charge 1 vortices: (a) charge = 1, (b) charge = 2, (c) charge = 3 (close-up view), (d) charge = 4 (close-up view).

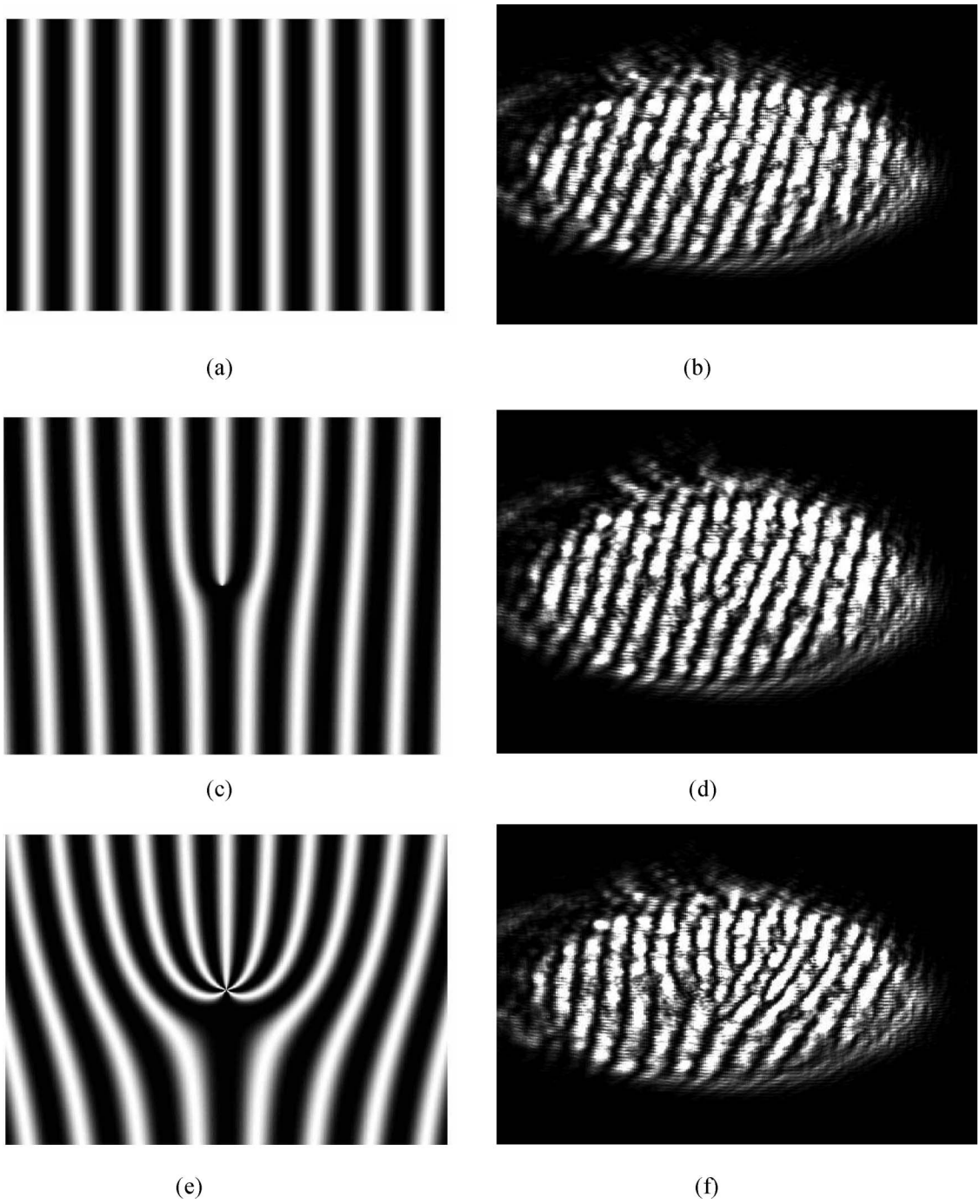

Fig. 6. Interference pattern [(a), (c), (e), simulated and (b), (d), (f), experimental] between reference plane wave and wave reflected off deformable mirror illustrating fork patterns due to the phase singularities present in the beam. (a) Simulated interference flat mirror, (b) experimental interference flat mirror, (c) simulated interference charge 1 vortex, (d) experimental interference charge 1 vortex, (e) simulated interference charge 5 vortex, (f) experimental interference charge 5 vortex.

from the periphery along the radial phase discontinuity to the central area of the beam.

4. Conclusion

We made use of the discontinuous surface of a segmented DM to create an optical vortex that, by definition, requires a phase discontinuity. The reflective surface allows for generation of vortices of any wavelength and the simple open-loop nature of the controller allows for integer and fractional vortex charge at any wavelength.

The authors wish to thank Michael A. Helmbrecht and Iris AO, Inc., for their support and for providing the deformable mirror.

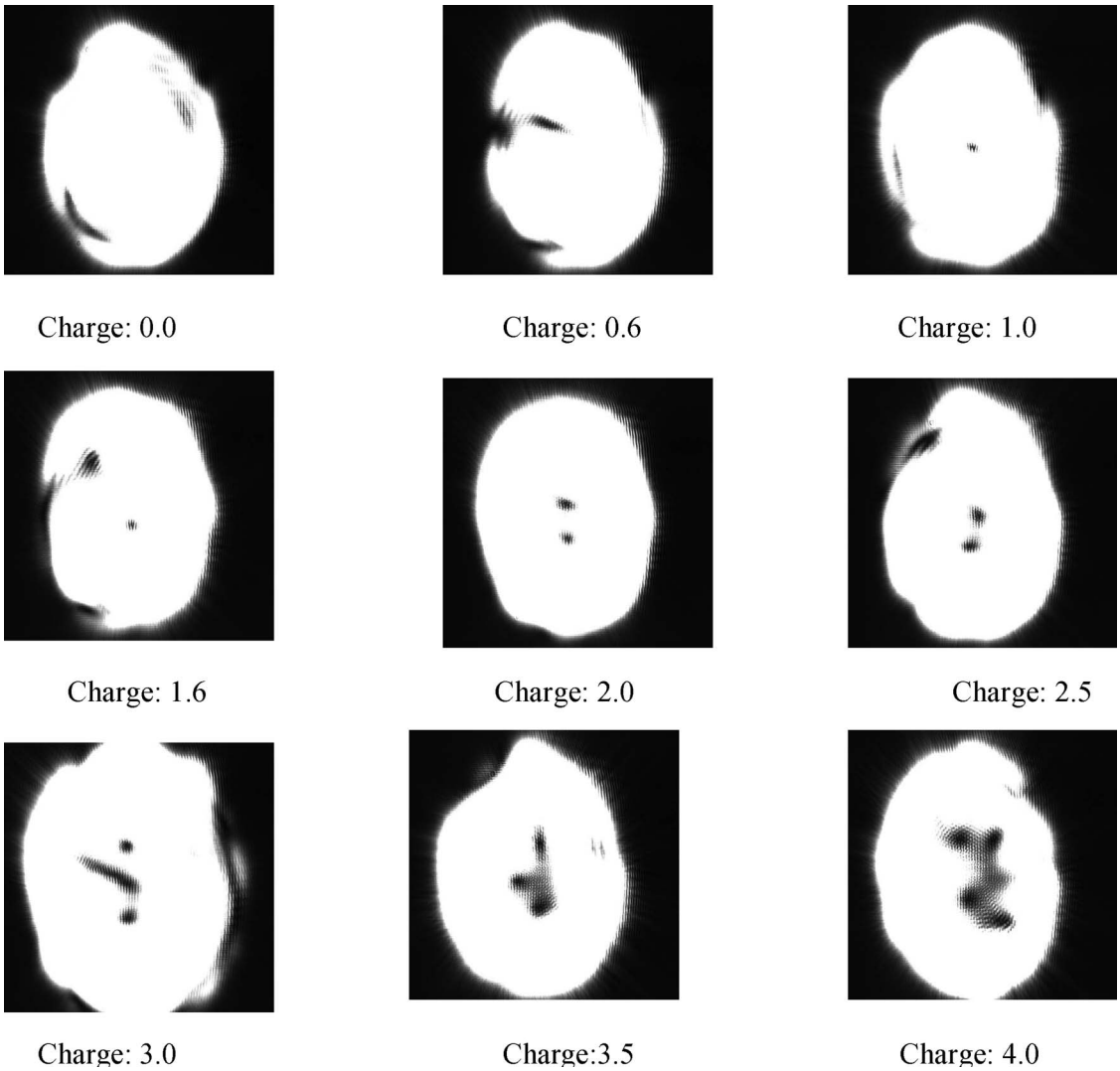

Fig. 7. Evolution of the intensity pattern for the beam reflected off the deformable mirror from charge 0.0 to charge 4.0 obtained by gradually increasing the phase discontinuity.

References

1. N. B. Baranova and B. Ya. Zel'dovich, "Dislocations of the wave-front surface and zeros of the amplitude," Zh. Eksp. Teor. Fiz. **80**, 1789–1797 (1981).
2. V. Basistiy, M. S. Soskin, and M. V. Vasnetsov, "Optical wavefront dislocations and their properties," Opt. Commun. **119**, 604–612 (1995).
3. V. Y. Bazhenov, M. V. Vasnetsov, and M. S. Soskin, "Laser beams with screw dislocations in their wavefronts," JETP Lett. **52**, 429–431 (1990).
4. N. B. Simpson, L. Allen, and M. J. Padgett, "Optical tweezers and optical spanners with Laguerre–Gaussian modes," J. Mod. Opt. **43**, 2485–2491 (1996).
5. J. E. Curtis, B. A. Koss, and D. G. Grier, "Dynamic holographic optical tweezers," Opt. Commun. **207**, 169–175 (2002).
6. J. E. Curtis and D. G. Grier, "Modulated optical vortices," Opt. Lett. **28**, 872–874 (2003).
7. Spalding, H. Melville, W. Sibbett, and K. Dholakia, "Applications of spatial light modulators in atom optics," Opt. Express **11**, 158–166 (2003).
8. G. Gibson, J. Courtial, M. Padgett, M. Vasnetsov, V. Pas'ko, S. Barnett, and S. Franke-Arnold, "Free-space information transfer using light beams carrying orbital angular momentum," Opt. Express **12**, 5448–5456 (2004).
9. Z. Bouchal and R. Celechovsky, "Mixed vortex states of light as information carriers," New J. Phys. **6**, 131–145 (2004).
10. R. Čelechovský and Z. Bouchal, "Optical implementation of the vortex information channel," New J. Phys. **9**, 328 (2007).
11. C. Paterson, "Atmospheric turbulence and orbital angular momentum of single photons for optical communication," Phys. Rev. Lett. **94**, 153901 (2005).
12. G. Gbur and R. K. Tyson, "Vortex beam propagation through atmospheric turbulence and topological charge conservation," J. Opt. Soc. Am. A **25**, 225–230 (2008).
13. M. V. Vasnetsov, I. G. Marienko, and M. S. Soskin, "Self-reconstruction of an optical vortex," JETP Lett. **71**, 130–133 (2000).
14. M. Scipioni, "Propagation of optical vortices through fog," M.S. thesis (University of North Carolina at Charlotte, 2004).
15. D. McGloin, G. D. P. Rhodes, D. M. Gherardi, J. Livesey, D. McGloin, H. Melville, T. Freegarde, and K. Dholakia, "Atom guiding along high order Laguerre–Gaussian light beams formed by spatial light modulation," J. Mod. Opt. **53**, 547–556 (2006).
16. N. R. Heckenberg, R. McDuff, C. P. Smith, and A. G. White, "Generation of optical phase singularities by computer-generated holograms," Opt. Lett. **17**, 221–223 (1992).

17. J. Courtial and M. J. Padgett, "Performance of cylindrical lens mode converter for producing Laguerre–Gaussian modes," Opt. Commun. **159**, 13–18 (1999).
18. D. Pal Ghai, P. Senthilkumaran, and R. S. Sirohi, "Adaptive helical mirror for generation of optical phase singularity," Appl. Opt. **47**, 1378–1383 (2008).
19. Y. Izdebskaya, V. Shvedov, and A. Volyar, "Generation of higher-order optical vortices by a dielectric wedge," Opt. Lett. **30**, 2472–2474 (2005).
20. X. C. Yuan, B. P. S. Ahluwalia, S. H. Tao, W. C. Cheong, L. S. Zhang, J. Lin, J. Bu, and R. E. Burge, "Wavelength-scalable micro-fabricated wedge for generation of optical vortex beam in optical manipulation," Appl. Phys. B **86**, 209–213 (2007).
21. C. Rotschild, S. Zommer, S. Moed, O. Hershcovitz, and S. G. Lipson, "Adjustable spiral phase plate," Appl. Opt. **43**, 2397–2399 (2004).
22. V. V. Kotlyar, A. A. Almazov, S. N. Khonina, V. A. Soifer, H. Elfstrom, and J. Turunen, "Generation of phase singularity through diffracting a plane or Gaussian beam by a spiral phase plate," J. Opt. Soc. Am. A **22**, 849–861 (2005).
23. C. S. Guo, D. M. Xue, Y. J. Han, and J. Ding, "Optimal phase steps of multi-level spiral phase plates," Opt. Commun. **268**, 235–239 (2006).
24. S. S. R. Oemrawsingh, J. A. W. van Houwelingen, E. R. Eliel, J. P. Woerdman, E. J. K. Verstegen, J. G. Kloosterboer, and G. W. 't Hooft, "Production and characterization of spiral phase plates for optical wavelengths," Appl. Opt. **43**, 688–694 (2004).
25. K. J. Moh, X.-C. Yuan, W. C. Cheong, L. S. Zhang, J. Lin, B. P. S. Ahluwalia, and H. Wang, "High-power efficient multiple optical vortices in a single beam generated by a kinoform-type spiral phase plate," Appl. Opt. **45**, 1153–1161 (2006).
26. J. Lin, X. Yuan, S. H. Tao, and R. E. Burge, "Synthesis of multiple collinear helical modes generated by a phase-only element," J. Opt. Soc. Am. A **23**, 1214–1218 (2006).
27. M. A. Helmbrecht, T. Juneau, M. Hart, and N. Doble, "Segmented MEMS deformable-mirror technology for space applications," Proc. SPIE **6223**, 622305 (2006).
28. Jonathan Leach, Eric Yao, and Miles J. Padgett, "Observation of the vortex structure of a non-integer vortex beam," New J. Phys. **6**, 71–78 (2004).
29. S. S. R. Oemrawsingh, E. R. Eliel, J. P. Woerdman, J. K. Verstegen, J. G. Kloosterboer, and G. W. 't Hooft, "Half integral spiral phase plates for optical wavelengths," J. Opt. A **6**, S288–S290 (2004).
30. W. M. Lee, X.-C. Yuan, and K. Dholakia, "Experimental observation of optical vortex evolution in a Gaussian beam with an embedded fractional phase step," Opt. Commun. **239**, 129 (2004).
31. V. Basistiy, V. A. Pas'ko, V. V. Slyusa, M. S. Soskin, and M. V. Vasnetsov, "Synthesis and analysis of optical vortices with fractional topological charges," J. Opt. A **6**, S166–S169 (2004).
32. M. V. Berry, "Optical vortices evolving from helicoidal integer and fractional phase steps," J. Opt. A **6**, 259–268 (2004).